

FREQUENCY CHARACTERISTICS OF AN ELECTODIFFUSION VELOCITY SENSOR

P. I. Geshev and A. I. Chernykh

UDC 536.252:532.517.6

The velocity sensor is a platinum wire 1, attached to glass 2 (Fig. 1). The essence of the electrodiffusion method of measurement is briefly as follows: A flux of electrolyte, containing two kinds of ions, e.g., $\text{Fe}(\text{CN})_6^{3-}$ and $\text{Fe}(\text{CN})_6^{4-}$, is incident on the sensor on its normal working surface; a rather large negative potential (0.4–0.8 V) is maintained on the platinum, leading to a charge exchange reaction between the three-charge ion and four-charge ion, $\text{Fe}(\text{CN})_6^{3-} + e^- \rightleftharpoons \text{Fe}(\text{CN})_6^{4-}$; this electrochemical reaction is remarkable in the fact that, of the oxidizing-regenerative reactions, it apparently has the largest rate and takes place so rapidly that the rate of change of current through the cathode is limited only by convective diffusion of the triple-charge ions to the electrode surface. The equation describing the ion diffusion process has the form

$$\frac{\partial c}{\partial t} + v(y, t) \frac{\partial c}{\partial y} = D \frac{\partial^2 c}{\partial y^2}, \quad (1)$$

where c is the concentration of ions vanishing at the electrode; D is the diffusion coefficient of these ions; and $v(y, t)$ is the velocity component of the liquid normal to the electrode surface and depending only on the time t and the coordinate y normal to the surface. The fact that Eq. (1) contains only the single coordinate y makes it a great deal simpler to construct a sensor theory. This property is known as the equi-admission property of the surface and also holds in the rotating-disk electrode method [1]. The presence of the velocity $v(y, t)$ in Eq. (1) means that the oncoming liquid velocity is related to the current through the cathode, and this is the principal basis for the method of measurement. A detailed description of the method is contained, e.g., in [2]. The method was used to investigate flows of rheologically complex media [3], and in liquid-gas flows [4].

Because of the low diffusion coefficient of the reacting ions ($D \sim 10^{-10} \text{ m}^2/\text{c}$) the electrode diffusion method has inertia, on the order of the expected inertia of a thermal anemometer [2]. The amplitude loss and the inertial phase delay of high-frequency fluctuations can be calculated and corrected if one knows the frequency characteristic (FC) of the sensor $H(i\omega)$, defined as the ratio of the complex amplitude of the harmonic signal at the exit $\tilde{i}(\omega)$ (current) to the "signal" amplitude at the "input" (velocity). It is convenient to consider the FC as dimensionless and normalized to unity at zero frequency

$$H(i\omega) = \frac{\tilde{i}(\omega) \tilde{w}(0)}{\tilde{i}(0) \tilde{w}(\omega)}. \quad (2)$$

In this form the FC can be used as a direct measure of the inertia of the sensor at frequency ω . The FC makes sense only for linear systems. This means that in calculations one must assume that the velocity and concentration fluctuations are small and must linearize the system of equations describing the sensor operation. The condition for velocity fluctuation amplitude to be small usually holds in actual experiments.

In deriving the system of sensor equations the following assumptions are made: 1) The Reynolds number, based on the outer sensor diameter d , is quite large, and the approximation of boundary layer theory are valid. 2) The electrode occupies only a small area near the stagnation point, so that the components of radial and normal velocity in the boundary layer can be written in the form $u = r \partial f(y, t) / \partial y$, $v = -2f(y, t)$,

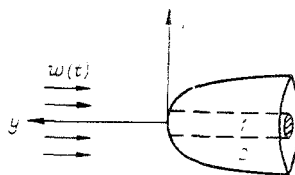


Fig. 1

Novosibirsk. Translated from Zhurnal Prikladnoi Mekhaniki i Tekhnicheskoi Fiziki, No. 4, pp. 78–82, July–August, 1979. Original article submitted June 29, 1978.

where r is the distance from the axis of symmetry; and $f(y, t)$ is the stream function for axisymmetric flow [5]. 3) The potential flow outside the boundary layer near the stagnation point is given by the formulas $U = kw(t)r/d$, $V = -2kw(t)y/d$, where $w(t)$ is the liquid velocity at large distance from the sensor ($y \gg d$); and k is some dimensionless constant on the order of unity, given in principle by an exact solution of the outer potential flow problem (for the body analyzed by Rankine [6], created by a source in a uniform flow, $k = 4$). This constant can be determined during sensor calibration. 4) It is assumed that the Schmidt number is large, $Sc = \nu/D \gg 1$ (ν is the kinematic viscosity of the liquid). In this case the diffusion boundary layer is less than the hydrodynamic boundary layer by a factor of $Sc^{1/3}$, and the velocity in it is given by the formula $v = -\partial^2 f(y, t)/\partial y^2|_{y=0} y^2$.

The equations for the average quantities and the linearized equations for the fluctuations are obtained from the Navier-Stokes equations and Eq. (1)

$$f_0'' - 2f_0'f_0' - \nu f_0'''' = a_0^2; \quad (3)$$

$$b_0 y^2 c_0' + D c_0'' = 0; \quad (4)$$

$$\frac{\partial f_1}{\partial t} - 2f_0'f_1' - 2f_0''f_1 - 2f_1''f_0 - \nu f_1'''' = 2a_0 a_1 + \frac{da_1}{dt}; \quad (5)$$

$$\frac{\partial c_1}{\partial t} - b_0 y^2 c_1' - D c_1'' = b_1 y^2 c_0'; \quad (6)$$

where the subscripts 0 and 1 denote, respectively, steady-state and fluctuating quantities; the primes for the functions denote differentiation with respect to y , and the notation has been used: $a_0 = kw_0/d$; $a_1 = kw_1(t)/d$; $b_0 = f_0''(y=0)$; $b_1 = f_1''(y=0, t)$ (w_0 and $w_1(t)$ are the average and fluctuating velocity at infinity). The boundary conditions for Eqs. (3)-(6) have the form

$$f_0 = f_0' = f_1 = f_1' = 0, \quad c_0 = c_1 = 0 \quad \text{for } y = 0; \quad (7)$$

$$f_0' = a_0, \quad f_1' = a_1, \quad c_0 = c_\infty, \quad c_1 = 0 \quad \text{for } y = \infty. \quad (8)$$

Equations (3) and (4) have known solutions (see, e.g., [5]). Equations (5) and (6) can be integrated as the equations of two sequentially coupled subsystems. The first subsystem is the hydrodynamic boundary layer, at the inlet to which (on the right in Eq. (5)) are given the velocity fluctuations $w_1(t)$ and at the "exit" we obtain the values $b_1 = f_1''(y=0)$. The second subsystem describes the diffusion boundary layer: At the "inlet" we are given the quantity b_1 , and at the "exit" the mass flux which also determines the current through the electrode, according to the Faraday law: $i_1 = -FSD c_1'(y=0; t)$, where F is the Faraday number; and S is the cathode area. It is clear that the FC for the whole system is equal to the product of the FCs of the subsystems.

We shall take only one harmonic from the velocity fluctuation spectrum $a_1(t) = \tilde{a}_1 e^{i\omega t}$; because of the subsystem linearity we have $f_1(t) = \tilde{f}_1 e^{i\omega t}$, $c_1(t) = \tilde{c}_1 e^{i\omega t}$, where $\tilde{a}_1, \tilde{f}_1, \tilde{c}_1$ are the complex amplitudes of the corresponding fluctuations.

We introduce the dimensionless variables

$$\eta_+ = \left(\frac{a_0}{\nu}\right)^{1/2} y, \quad \varphi_0(\eta_+) = \frac{f_0}{a_0}, \quad \varphi_1(\eta_+) = \frac{\tilde{f}_1}{a_1}, \quad \omega_+ = \frac{\omega}{a_0};$$

$$\eta_- = \left(\frac{b_0}{D}\right)^{1/3} y, \quad \psi_0(\eta_-) = \frac{c_0}{c_\infty}, \quad \psi_1(\eta_-) = \frac{b_0 \tilde{c}_1}{\tilde{b}_1 c_\infty}, \quad \omega_- = \left(\frac{\nu}{D}\right)^{1/3} \frac{\omega}{a_0},$$

where c_∞ is the ion concentration at infinity; and $\tilde{b}_1 = \tilde{f}_1''(y=0)$. In these variables the equations and the boundary conditions have the form

$$\varphi_0'' - \varphi_0' \int_0^{\eta_+} \varphi_0' d\eta_+ - \varphi_0'''' = 1; \quad (9)$$

$$\eta_-^2 \psi_0' + \psi_0'' = 0; \quad (10)$$

$$i\omega_+ \varphi - 2\varphi_0' \varphi - 2\varphi_0'' \int_0^{\eta_+} \varphi d\eta_+ - 2\varphi_0' \int_0^{\eta_-} \varphi_0' d\eta_+ - \varphi'' = 2 + i\omega_+; \quad (11)$$

$$i0.834\omega_- \psi - \eta_-^2 \psi' - \psi'' = \eta_-^2 \psi_0'; \quad (12)$$

$$\varphi_0 = \varphi = \psi_0 = \psi = 0 \quad \text{for } \eta_{+,-} = 0; \quad (13)$$

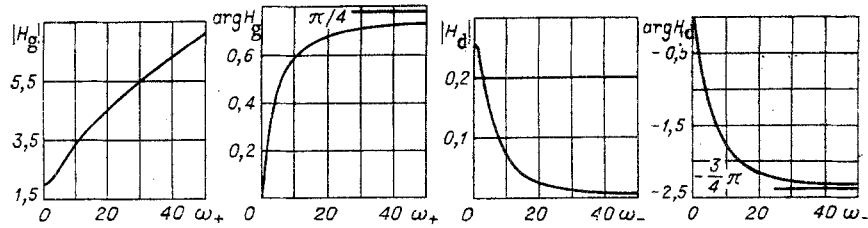


Fig. 2

$$\varphi_0 = \varphi = \psi_0 = 1, \quad \psi = 0 \quad \text{for } \eta_{+,-} = \infty. \quad (14)$$

At the lower limit of the integrals in Eqs. (9) and (11) we apply the condition of Eq. (7). The primes in Eqs. (9)–(12) now denote differentiation with respect to the corresponding argument η_+ or η_- . Calculations show that $\varphi'_0(\eta_+ = 0) = 1.312$; this is in complete agreement with the value from [5]. For convenience the numerical coefficient $0.834 = 1.312^{-2/3}$ is left in Eq. (12) and is not introduced into ω_- .

Equation (10) is integrated analytically. The numerical solution of the remaining equations in Eqs. (9)–(12) is obtained by the time-dependent method. To do this we introduce derivatives with respect to the desired function on the left side of the equations relative to some fictitious time τ , and with an implicit difference scheme we find the corresponding solutions which are steady-state with respect to τ , corresponding to a given frequency.

As a result we obtain two complex functions $H_g = \varphi'(\eta_+ = 0)$ and $H_d = \psi'(\eta_- = 0)$, depending only on ω_+ and ω_- and which are dimensionless and which are not normalized to the FC subsystems. The moduli and arguments of these functions are shown in Fig. 2 (the straight lines are the asymptotic values of the arguments for $\omega_{+,-} \rightarrow \infty$).

The correctness of the numerical results is confirmed by comparing with the asymptotic formulas obtained in the limit as $\omega \rightarrow 0$ and $\omega \rightarrow \infty$, from Eqs. (11) and (12). The modulus of H_g deviates from the asymptotic formula by less than 1% even for $\omega_+ > 30$, while the same deviation of $|H_d|$ from the asymptotic value is reached only for $\omega_- > 100$. The asymptotic formulas are used for an accurate approximation to the results of the numerical computation

$$|H_g| = (15 + \omega_+^2)^{1/4}; \quad (15)$$

$$\arg H_g = 0.5 \arctg(0.256\omega_+); \quad (16)$$

$$|H_d| = 0.259 \left(\frac{1 + 2.32 \cdot 10^{-3} \omega_-^2}{1 + 4.45 \cdot 10^{-2} \omega_-^2 + 1.49 \cdot 10^{-4} \omega_-^4} \right)^{3/4}; \quad (17)$$

$$\arg H_d = -1.5 \arctg(0.241\omega_- (1 + 2.04 \cdot 10^{-3} \omega_-^2)). \quad (18)$$

The relative error in the approximation of Eqs. (15)–(18) does not exceed 0.5%.

We note an interesting feature of the hydrodynamic boundary layer. The modulus of H_g increases with frequency, and its argument is positive: The phase of the fluctuations at the "exit" leads the phase of the fluctuations at the "inlet." The quantity $b(t)$ is associated with friction near the stagnation point. In fact, the tangential friction stress is

$$\tau_w = \rho v (\partial u / \partial y)_{y=0} = \rho v r b(t),$$

and, as was shown in [5], the friction fluctuations lead the velocity fluctuations in phase, in the boundary layer. The FC of the diffusion boundary layer is normal: The high-frequency fluctuations are strongly suppressed in amplitude and are delayed in phase. The total FC of the electrode diffusion velocity sensor was calculated in [7], but only for certain values of Sc . The authors of that paper did not note that the total FC of the sensor is decomposed into the product of the two universal frequency functions. Comparison of our results with the values calculated in [7] showed that the FC moduli differ by no more than 3%, but that the difference in phases is as high as 7%. These rather large deviations are due, apparently, to an unsuccessful method of calculation used in [7], the method of "ranging," using the boundary conditions.

Using Eq. (2), we can now write a final formula for the modulus of the normalized FC of the velocity sensor

$$|H(i\omega)| = \left(1 + \frac{\omega_-^2}{15Sc^{2/3}}\right)^{1/4} \left(\frac{1 + 2.32 \cdot 10^{-3} \omega_-^2}{1 + 4.45 \cdot 10^{-3} \omega_-^2 + 1.49 \cdot 10^{-4} \omega_-^4}\right)^{3/4},$$

where $\omega_- = \frac{\omega d}{k w_0} \left(\frac{\nu}{D}\right)^{1/3}$.

The phase of the FC is defined as the sum of the phases in Eqs. (16) and (18). The error in the resulting formulas does not exceed 1%. These can be used to obtain the spectra and the individual cases of turbulent velocity fluctuations.

LITERATURE CITED

1. Yu. V. Pleskov and V. Yu. Filinovskii, *The Rotating Disk Electrode* [in Russian], Nauka, Moscow (1972).
2. T. Mizushina, "The electrochemical method in transport phenomena," in: *Advances in Heat Transfer*, Vol. 7, Academic Press (1971).
3. *Rheophysics, Collection of Papers*, Tr. ITMO Akad. Nauk BSSR, Minsk (1977).
4. A. P. Burdukov, B. K. Koz'menko, and V. E. Nakoryadov, "Distribution of liquid phase velocity profiles in a gas-liquid flow at low gas content," *Zh. Prikl. Mekh. Tekh. Fiz.*, No 6 (1975).
5. H. Schlichting and Kestin, *Boundary Layer Theory*, McGraw-Hill (1968).
6. L. M. Milne-Thomson, *Theoretical Hydrodynamics*, Crane Russak (1976).
7. Yu. E. Bogolyubov and L. P. Smirnova, "Mass emission near the stagnation point in a fluctuating flow," *Izv. Sib. Ord. Akad. Nauk SSSR*, No. 8, Part 2 (1977).

EXPERIMENTAL INVESTIGATION OF SONIC AND SUPERSONIC ANNULAR JETS

M. A. Koval' and A. I. Shvets

UDC 533.695.7

A considerable number of theoretical and experimental reports, which are surveyed in [1, 2], e.g., have been devoted to the investigation of flow in supersonic annular jets. The influence of the Mach number of the jet and the expansion ratio on the value of the base pressure has been established experimentally and the principal modes of flow in annular jets have been determined. Until now, however, the influence of the relative sizes of annular nozzles and of the profiling of the flow-through part on the flow has been little studied, in connection with which the present work was performed. Comparisons are made of the expansion ratio of the escaping jet, the wave structure, and the pressure in the base region.

The flow in three sonic and three supersonic jets escaping from annular nozzles with plane cuts was investigated experimentally. The subsonic flow channels in the nozzles provided for not less than fivefold compression of the stream and were profiled in such a way that a uniform stream was assured in the throats of the supersonic nozzles or at the cuts of the sonic nozzles. In the exit cross sections of the sonic nozzles the ratio of the inner to the outer diameter was $d/D = 0.5, 0.75, \text{ and } 0.9$ (Fig. 1). The supersonic channels were conical, and the nozzles had the following parameters: $d/D = 0.6; \mu = 15^\circ; \beta = 24^\circ; M_a = 2.63; d/D = 0.68; \mu = 10^\circ; \beta = 6^\circ; M_a = 1.8; d/D = 0.91; \mu = 10^\circ; \beta = 10^\circ; M_a = 2.78$ (M_a is the rated Mach number of the nozzle).

1. Pressure in Base Region

In order to study the influence of the relative diameter of a nozzle on the relative base pressure $p_1 = p_{p0}/p_\infty$ measured at the axis of the nozzle face (the index b is for the base cut, 0 for the nozzle axis, and ∞ for parameters of the flooded space into which the jet discharges), in Fig. 1 we give the dependence $p_1 = f(n)$ for the three sonic jets and one of the supersonic ones ($M_a = 1: d/D = 0.9$ (1, 2), $d/D = 0.75$ (3, 4) $d/D = 0.5$ (5, 6); $M_a = 2.63, \mu = 15^\circ, \beta = 24^\circ: d/D = 0.6$ (7)). Since the expansion ratio of a sonic jet cannot be less than $n = 1$ ($n = p_a/p_\infty$, where p_a is the pressure at the nozzle cut), the quantity $n' = p_a M_a^2/p_\infty$ is taken as

Kharkov, Moscow. Translated from *Zhurnal Prikladnoi Mekhaniki i Tekhnicheskoi Fiziki*, No. 4, pp. 83-89, July-August, 1979. Original article submitted May 26, 1978.